



Cite this: *Soft Matter*, 2022, 18, 5014

Received 28th April 2022,  
Accepted 28th June 2022

DOI: 10.1039/d2sm00543c

[rsc.li/soft-matter-journal](http://rsc.li/soft-matter-journal)

## A new order of liquids: polar order in nematic liquid crystals

Richard J. Mandle <sup>ab</sup>

Given the widespread adoption of display technology based on nematic liquid crystals, the discovery of new nematic phases at thermodynamic equilibrium, although extremely rare, generates much excitement. The remarkable discovery polar order and giant ferroelectric polarisation in a nematic fluid is a watershed moment in soft matter research, and is one of the most important discoveries in the 150 year history of liquid crystals. After a brief introduction to this emerging field, we present the current state-of-the-art in terms of understanding the molecular origins of this phase, before exploring how molecular structure underpins the incidence of this phase, as well as exploring future directions.

### Introduction

Nematic liquid crystals are ubiquitous in our daily lives thanks to their widespread adoption in display technology.<sup>1</sup> The nematic phase is characterised by its constituent molecules (or particles) having – on average – a preferred direction of orientation, which is termed the director. As with virtually all fluid phases of matter at equilibrium, the bulk nematic liquid crystals we encounter day-to-day are apolar, irrespective of their molecular polarity. In other words, despite their bulk orientational order, the constituent particles display no preference for orientation parallel or antiparallel to the director (Fig. 1(a)), and molecules have an equal probability of being aligned parallel or antiparallel to the director.

A nematic phases with polar order (Fig. 1(b)) has recently realised experimentally, presenting an interesting counterpoint to the apolar nematics we encounter daily. In 1916 Max Born speculated that a polar (and thus ferroelectric) fluid would exist if the molecular electric dipole moments are large enough that dipole–dipole interactions between molecules are sufficient to overcome thermal fluctuations.<sup>2</sup> The push to develop and deploy apolar nematic liquid crystals in display technology, coupled with the absence of experimental proof of the existence of polar nematic phases, meant that Born's conjecture was seemingly forgotten by experimentalists. Frank<sup>3</sup> and Brand<sup>4</sup> made theoretical arguments to show that, for polar nematics, spontaneous splay deformation provides a means to escape polar order.

In 2017 two materials were reported – RM734<sup>5</sup> and DIO<sup>6</sup> – that are now understood to have polar nematic order and are

ferroelectric, over a century after Born's conjecture.<sup>7–9</sup> This so-called ferroelectric nematic ( $N_F$ ) phase displays a slew of unique properties: ferroelectric properties with huge spontaneous polarisation,<sup>8,10</sup> polar domains,<sup>10</sup> strong non-linear optical response,<sup>11</sup> unique electrooptic responses,<sup>12</sup> and thermal gradient-induced circular motion of particles,<sup>13</sup> to name a few. The remarkable properties of the  $N_F$  phase, coupled with fluidity and relative ease of alignment,<sup>14</sup> will ensure this field flourishes in the decades to come.<sup>15</sup> Progress in understanding and exploiting the unique physics of the  $N_F$  phase is reliant on the design and synthesis of new materials, an area that has undergone significant progress in the since the report of the first polar nematic materials in 2017,<sup>5,6,16</sup> and this is the focus of this article.

### Archetypal materials

The archetypal  $N_F$  materials are RM734<sup>5</sup> and DIO,<sup>6</sup> shown in Fig. 1(a), both being reported almost simultaneously in 2017 by Mandle *et al.* (RM734) and Nishikawa *et al.* (DIO). In RM734 the orientation of the ester units coupled with the polarity of the terminal nitro group gives a dipole moment of  $\sim 11$  D (DFT:B3LYP/6-31G(d)). For DIO, the fluorine substitution pattern coupled with ester orientation and also 1,3-dioxanyl ring generate a dipole moment of  $\sim 9$  D (DFT:B3LYP/6-31G(d)).<sup>6</sup> In the  $N_F$  phase spontaneous polarisations of 6.0 and 3.8  $\mu\text{C cm}^{-2}$  have been measured for RM734 and DIO, respectively.<sup>6,8</sup>

For apolar nematics, the introduction of chirality causes the nematic director to rotate, giving a chiral nematic phase ( $N^*$ ) which has a helical superstructure (Fig. 1(d)), with the director oriented perpendicular to the helical axis. Notably, the polar analogue of the chiral nematic phase has very recently been discovered.<sup>17–21</sup> Lastly, one further example of nematic polymorphism must be considered. In 2011 the twist-bend nematic

<sup>a</sup> School of Physics and Astronomy, University of Leeds, UK LS2 9JT

<sup>b</sup> School of Chemistry, University of Leeds, UK LS2 9HT.

E-mail: [r.mandle@leeds.ac.uk](mailto:r.mandle@leeds.ac.uk)



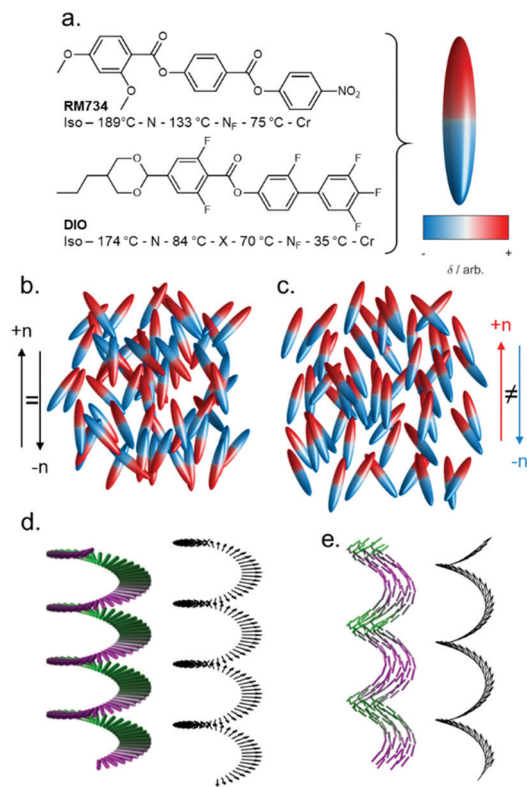


**Fig. 1** Nematic polymorphism: (a) molecular structures of RM734 and DIO, with transition temperatures (°C),<sup>5,6</sup> and polar ellipsoid representation used elsewhere in this figure. Programmatically generated cartoon depictions of ellipsoids forming a conventional apolar nematic phase (b) and polar nematic phase (c), with order parameters ( $\langle P_2 \rangle$ ) of 0.60 and 0.67, respectively. Cartoon depictions of the precession of the nematic director in the helical chiral nematic phase (d) and heliconical twist-bend nematic phase (e).

phase was discovered, having been predicted some ten years earlier by Ivan Dozov, marking the first new nematic phase type

discovered in over half a century.<sup>22–24</sup> It has been suggested that a polar twisted model of the heliconical N<sub>TB</sub> phase, the so-called N<sub>PT</sub> model, is a better descriptor;<sup>25</sup> we note that such an N<sub>PT</sub> phase is to the ferroelectric nematic phase what the N<sub>TB</sub> phase is to the conventional nematic.

## Materials and the incidence of the N<sub>F</sub> phase

We now focus on structural variations, highlighting how changes in molecular structure affect the transition temperatures of each material. We start by considering derivatives of RM230, purely as this was the first reported N<sub>F</sub> material that we are aware of, albeit assigned as an “unknown nematic” (N<sub>X</sub>) at the time.<sup>16</sup> Confounding our initial expectations, the presence of longer terminal chains eliminates the N<sub>F</sub> phase, yet shortening the terminal chain to methoxy (to give RM734) gives a large (~50 °C) enhancement to T<sub>N<sub>F</sub>-N</sub>.<sup>5</sup> A bulky lateral group is essential for the formation of the N<sub>F</sub> phase in the RM-type materials; the group does not simply inhibit crystallisation, and removal of the lateral group decreases T<sub>N<sub>F</sub>-N</sub> by over 100 °C. A few variants of RM230 with alternate polar units were synthesised; incorporation of fluorine *ortho* to the terminal nitro group boosts T<sub>N<sub>F</sub>-N</sub> by over 30 °C. Conversely, replacement of nitro with nitrile suppresses the formation of the N<sub>F</sub> phase, as does the replacement of the 4-((4-nitrophenyl)benzoyl)benzoate core but lacking the lateral unit, exhibit the re-entrant N-SmA-N phase sequence rather than the N<sub>F</sub> phase.<sup>26,27</sup>

Of all of the variants of RM230 encountered so far, RM734, which features a 2,4-dimethoxybenzoate head group, has the ‘best’ transition temperatures. A number of alternate polar groups were explored by Mandle *et al.*<sup>5</sup> the 3-fluoro-4-nitrophenyl unit gives a small enhancement in T<sub>N<sub>F</sub>-N</sub> and notable reduction in T<sub>N-Iso</sub>. As

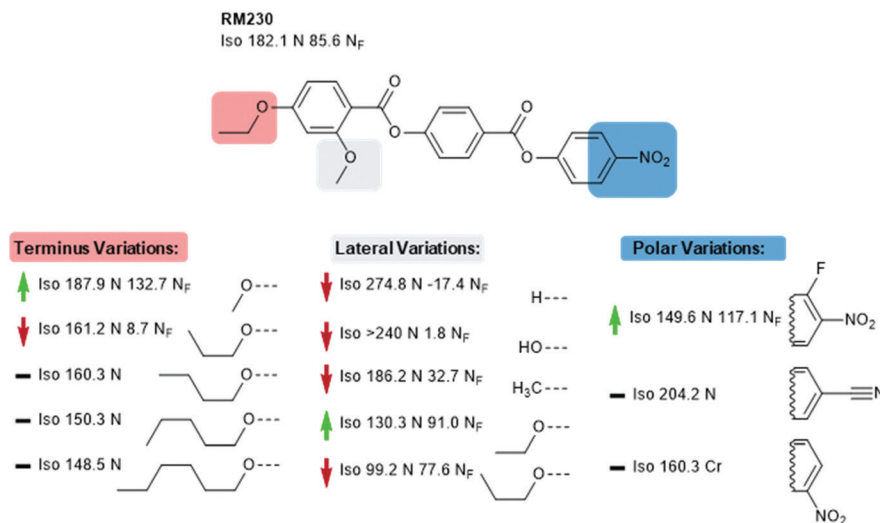


**Fig. 2** Structural variants of RM230: transition temperatures (°C) are on cooling from the isotropic liquid.<sup>5,16,21</sup> A green and red arrows indicate increased and decreased T<sub>N<sub>F</sub>-N</sub> relative to the parent material, respectively, while a black dash indicates the absence of the N<sub>F</sub> phase.



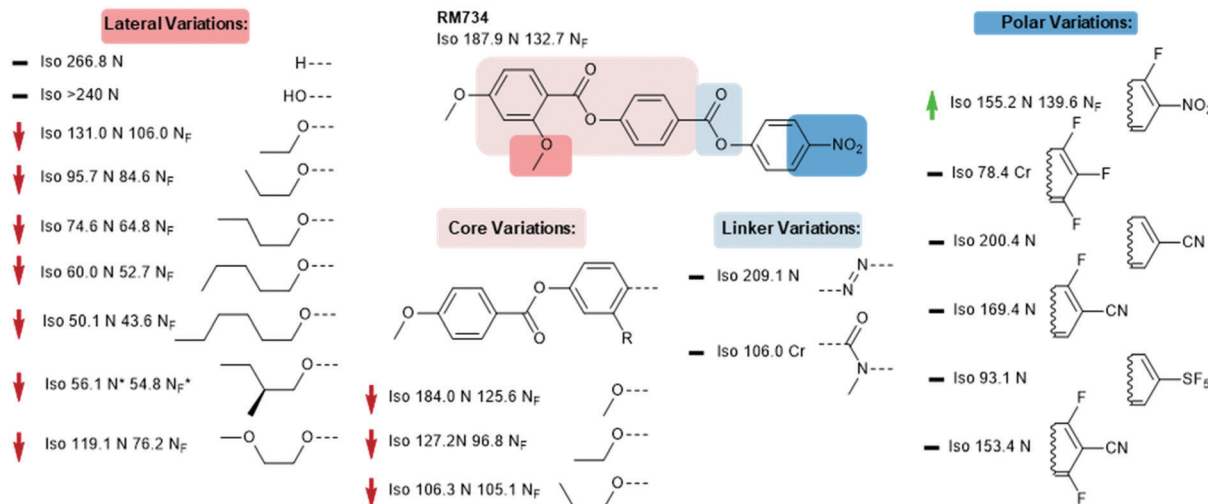


Fig. 3 Structural variants of RM734 temperatures ( $^{\circ}\text{C}$ ) are on cooling from the isotropic liquid.<sup>5,18,20,28</sup> A green and red arrows indicate increased and decreased  $T_{\text{NF-N}}$  relative to the parent material, respectively, while a black dash indicates the absence of the  $N_{\text{F}}$  phase.

will be shown later, fluorination is a viable strategy for enhancing  $T_{\text{NF-N}}$  in this class of materials, presumably *via* increased dipole-dipole interactions. Other polar units, shown in Fig. 3, were found to eliminate the  $N_{\text{F}}$  phase. Aya *et al.* reported a number of further variations to the RM734 core structure. Elongation of the lateral methoxy unit reduces  $T_{\text{NF-N}}$  relative to RM734, however melting points and clearing points are also reduced.<sup>28</sup> Imrie *et al.* also reported a number of RM734 derivatives with alternate lateral groups, including the (*S*)-2-methylbutoxy group which leads to the chiral  $N_{\text{F}}$  phase,<sup>20</sup> with this material also being reported independently by others.<sup>18</sup> Again, the increased steric bulk of these lateral groups depresses  $T_{\text{NF-N}}$  when compared to the parent material. Aya *et al.* synthesised materials in which the lateral unit is positioned to the central phenyl ring, all of which generate the  $N_{\text{F}}$  phase with a modest reduction in  $T_{\text{NF-N}}$ .<sup>28</sup> Use of azo or *n*-methylamide linking units eliminates the  $N_{\text{F}}$  phase entirely, and also the nematic phase in the case of the amide.<sup>28</sup>

As already shown for RM230 and RM734 (Fig. 2 and 3, respectively), fluorination *ortho* to the nitro unit gives notable increases in the onset temperature of the  $N_{\text{F}}$  phase while also depressing the clearing point slightly.<sup>5</sup> Jakli *et al.* reported a fluorinated variant of RM734 (known as RT11001, Fig. 4) in which a fluorine atom is positioned in the 3-position of the central ring.<sup>29</sup> The increase in molecular dipole moment leads to a large increase in spontaneous polarisation, with the reported value of  $6.9 \mu\text{C cm}^{-2}$  being the largest ever reported for a liquid crystalline system. Imrie *et al.*<sup>30</sup> provided further examples of fluorinated RM734 derivatives, finding one material that exhibits a direct isotropic to  $N_{\text{F}}$  phase transition (Fig. 4).

The material commonly known as DIO was reported virtually the same time as the RM-type materials; the combination of a 1,3-dioxane ring, carboxylate ester, and aromatic fluorination pattern gives a large longitudinal electric dipole moment. Although less well explored than the RM-type materials, a number of structural variations on this core structure are known. Increasing the molecular dipole moment by replacing

the monofluorophenyl with 2,6-difluorophenyl gives a large ( $> 50^{\circ}\text{C}$ ) increase in the onset temperature of the  $N_{\text{F}}$  phase; conversely, replacement with a 2-methoxyphenyl unit reduces  $T_{\text{NF-N}}$  slightly, while replacement with an unsubstituted benzene ring eliminates the  $N_{\text{F}}$  phase entirely.<sup>28</sup> Replacement of the ester unit of DIO with the geminal difluoromethyl unit (and also shortening of the terminal chain from propyl to methyl) eliminates the  $N_{\text{F}}$  phase, irrespective of the molecular structure at rings #3 and #4. In terms of their ability to generate the  $N_{\text{F}}$  phase this suggests that the  $\text{CF}_2\text{O}$  linking unit is inferior to an ester, however, as will be shown later, this unit has been utilised in ferroelectric nematic materials (Fig. 5).<sup>28</sup>

Li *et al.* recently reported a significant number of new  $N_{\text{F}}$  materials, many of which are homologous in structure with DIO with alternate polar functionalities and terminal chain lengths.<sup>33</sup> As a general trend, for a given core structure the shorter terminal chain lengths give the highest  $N_{\text{F}}$  onset temperature, mirroring the behaviour of the earlier RM230-like materials. The 4-cyano-2',3,5,6'-tetrafluorobiphenyl end

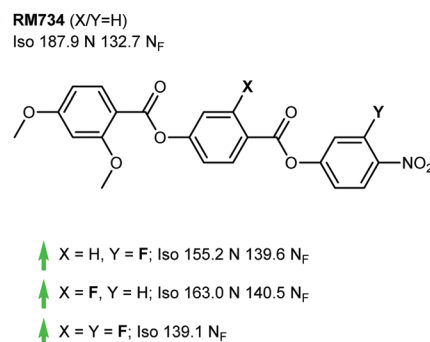


Fig. 4 Fluorinated derivatives of RM734; transition temperatures ( $^{\circ}\text{C}$ ) are on cooling from the isotropic liquid.<sup>5,29,30</sup> Green and red arrows indicate increased and decreased  $T_{\text{NF-N}}$  relative to the parent material, respectively, while a black dash indicates the absence of the  $N_{\text{F}}$  phase.



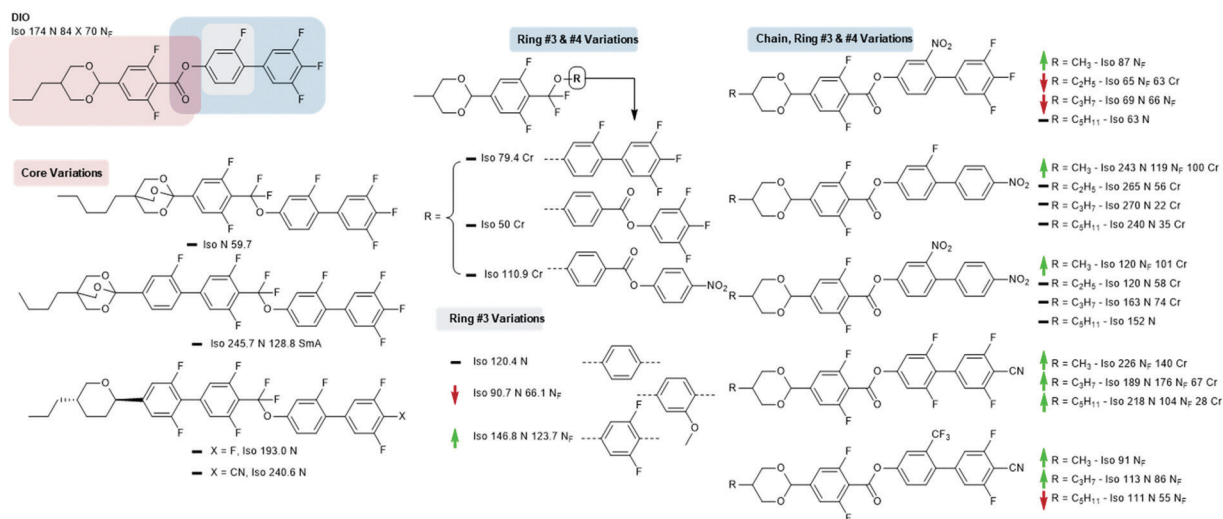


Fig. 5 Structural variants of DIO; transition temperatures ( $^{\circ}\text{C}$ ) are on cooling from the isotropic liquid.<sup>28,31–33</sup> Green and red arrows indicate increased and decreased  $T_{\text{NF-N}}$  relative to the parent material, respectively, while a black dash indicates the absence of the  $N_{\text{F}}$  phase.

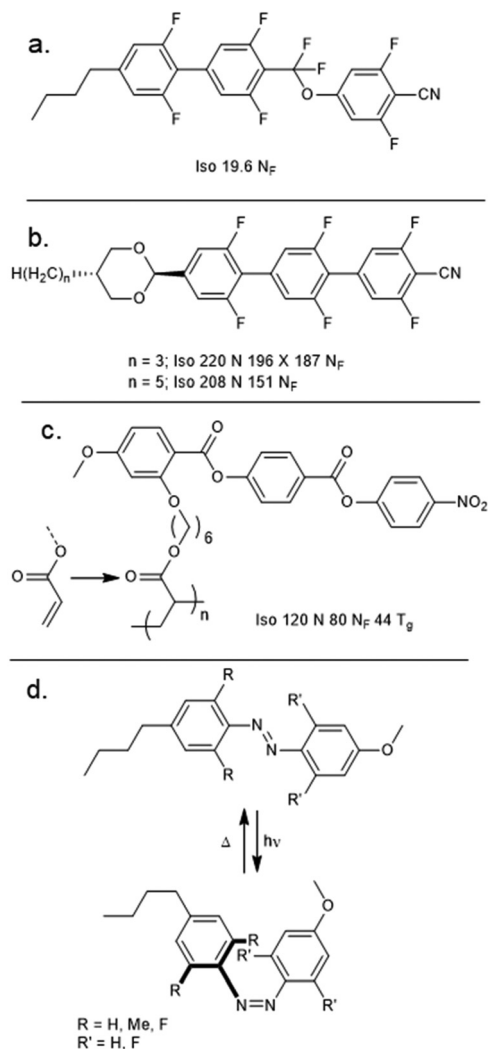


Fig. 6 Molecular structures and transition temperatures ( $^{\circ}\text{C}$ , on cooling) for some recent novel  $N_{\text{F}}$  materials (or additives).

group results in a remarkable increase in the onset temperature of the  $N_{\text{F}}$  phase; the onset temperature of the propyl derivative is over  $100^{\circ}\text{C}$  higher than that of DIO, with the methyl derivative being higher still. A smaller enhancement is found for the 4-cyano-3,5-difluoro-2'-trifluoromethylbiphenyl unit, while mono or dinitrated biphenyls are found to be largely inferior to DIO.

Examination of the patent literature reveals some orthoester 2,6,9-trioxabicyclo-(2.2.2)-octane derivatives (conveniently prepared *via* the action of boron trifluoride diethyl etherate on a suitable hydroxylmethyloxetane<sup>34</sup>) which are homologous in structure to DIO, although these materials are not reported to exhibit the  $N_{\text{F}}$  phase.<sup>31</sup> Some pyran homologues of DIO have been reported, and while these exhibit the conventional nematic phase the  $N_{\text{F}}$  is absent,<sup>32</sup> as is also the case for the closely related 1,3-dioxan-5-cyclobutyl and pyrrolidine homologues.<sup>35,36</sup>

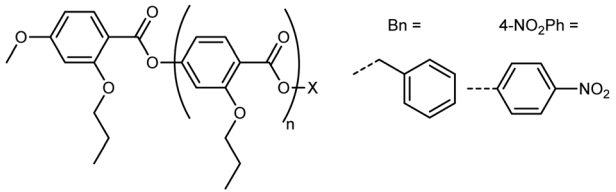
This brings us to an important point. The properties of novel LC materials are routinely measured as low concentration solutions in off-the-shelf nematic hosts, rather than as pure materials. Ordinarily this is quite acceptable, however in the case of the  $N_{\text{F}}$  phase this masks the polar order and gives only a conventional nematic phase. Therefore it seems reasonable to this author that there could exist a substantial pool of materials that exhibit the  $N_{\text{F}}$  phase yet have not been characterised as such. Fortunately, methods have been developed that enable rapid identification of the ferroelectric nematic *via* microscopy,<sup>37</sup> and this would appear to be an attractive direction for future studies.

## Emerging material classes

Bremer *et al.* described a material (UUQU-4-N, Fig. 6(a)) which undergoes a direct Isotropic to  $N_{\text{F}}$  transition.<sup>38</sup> Although the  $N_{\text{F}}$  phase is monotropic, the melting point of this material is sufficiently low as to permit room temperature studies on the



**Table 1** Transition temperatures ( $T/^\circ\text{C}$ ) of the 1st cooling cycle (DSC) for the  $\text{Bn}_{(n)}$  and  $\text{Nt}_{(n)}$  oligomers reported by Li *et al.*<sup>42</sup>



Name	X	$n$	$T_{\text{Cr}}$	$T_{\text{NF-Iso}}$
$\text{Bn}_2$	Bn	2	—	—
$\text{Bn}_3$	Bn	3	—	—
$\text{Bn}_4$	Bn	4	60	—
$\text{Bn}_6$	Bn	6	135	184
$\text{Bn}_8$	Bn	8	167	230
$\text{Bn}_{10}$	Bn	10	192	264
$\text{Bn}_{12}$	Bn	12	210	294
$\text{Nt}_1$	4- $\text{NO}_2\text{Ph}$	1	n/a	41
$\text{Nt}_2$	4- $\text{NO}_2\text{Ph}$	2	n/a	116
$\text{Nt}_3$	4- $\text{NO}_2\text{Ph}$	3	n/a	165
$\text{Nt}_4$	4- $\text{NO}_2\text{Ph}$	4	n/a	207
$\text{Nt}_6$	4- $\text{NO}_2\text{Ph}$	6	137	265
$\text{Nt}_8$	4- $\text{NO}_2\text{Ph}$	8	171	284

$\text{N}_F$  phase. Recently, Huang *et al.* have reported two highly fluorinated rod-like mesogens which exhibit the  $\text{N}_F$  phase (Fig. 6(b)).<sup>39</sup> As with all  $\text{N}_F$  materials known to date, these materials feature polar groups (in this case, 1,3-dioxane, 2,5-difluorophenyl, nitrile) oriented in such a way to give a large longitudinal molecular electric dipole moment. Although the high melting points of these materials render them somewhat impractical, the development of a new class of  $\text{N}_F$  materials is nonetheless extremely welcome.

Appending a pendant acrylate unit to the structure of RM734 enabled Dai *et al.* to perform *in situ* photopolymerisation, yielding the polymeric material SP1, which exhibits both

$\text{N}$  and  $\text{N}_F$  mesophases (Fig. 6(c)).<sup>40</sup> Positioning the pendant acrylate unit on other rings or in the terminal position of the monomer gave only a conventional nematic phase. More recently, Nishikawa *et al.* employed a photoisomerisable azobenzene additive (using DIO as a nematic host) to demonstrate a ferroelectric nematic material in which irradiation controls the dielectric permittivities (Fig. 6(d)),<sup>41</sup> demonstrating a photovisible capacitor which enables modulation of sound frequencies (in the range of 0.1–8.5 kHz).

Li *et al.* performed the precise synthesis of monodisperse 4-(2-propoxy)benzoate materials *via* the use of an orthogonal tetrahydropyranyl ether and benzyl ester protecting groups, to afford the benzyl terminated  $\text{Bn}_{(n)}$  materials and the 4-nitrophenyl terminated  $\text{Nt}_{(n)}$  materials.<sup>42</sup> The  $\text{Bn}_{(n)}$  and  $\text{Nt}_{(n)}$  materials can be considered as homologues of the poly(oxobenzoate) type liquid crystal polymers, and also to a lesser extent RM734 and its derivatives. Remarkably, the classical nematic phase is absent for all materials, with the formation of the  $\text{N}_F$  phase directly on cooling from the isotropic liquid demonstrated by both SHG and SHG-I microscopy. In the case of the  $\text{Bn}_{(n)}$  materials, the molecular dipole moment is generated almost entirely by the complementary orientation of ester linking units, and this affords a ferroelectric nematic phase albeit with a somewhat lower  $T_{\text{NF-Iso}}$  than the equivalent length nitro-terminated material. The discovery of the  $\text{N}_F$  phase in these systems demands that other oligo/poly(oxobenzoate) materials be reinvestigated as candidate ferroelectric nematics (Table 1).

Finally, we revisit the 4-cyano-3,5-difluoro terminated derivative of RM734, which we will refer to as RM734-CN(2F). Li *et al.* recently reported the synthesis of a large number of materials which derive from and expand upon the basic structure of RM734-CN(2F). Careful positioning of multiple fluorine atoms and/or replacement of the lateral methoxy unit with a trifluoromethyl enabled them to engineer materials which

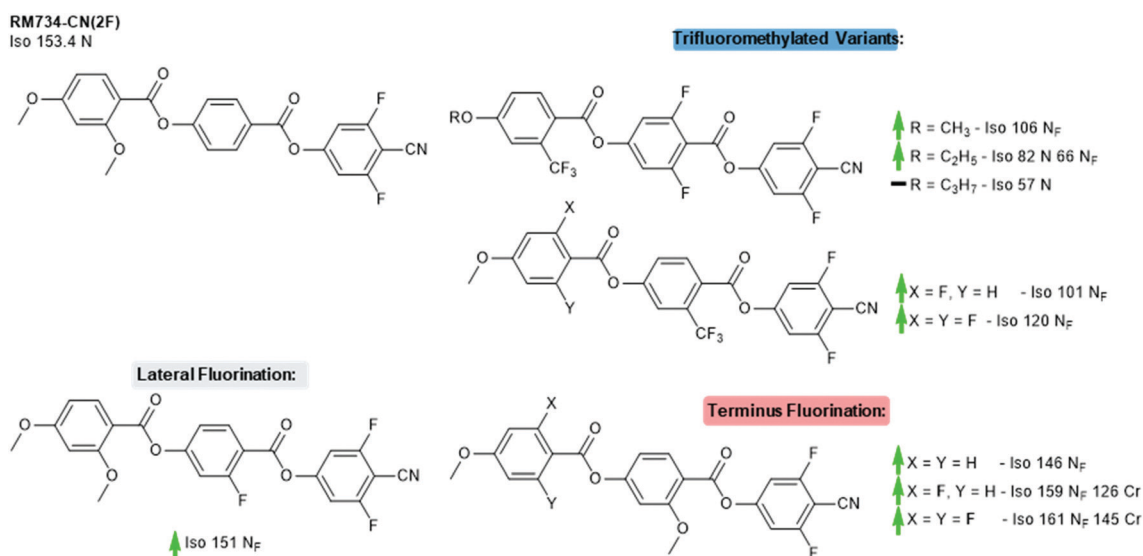


**Fig. 7** Structural variants of RM734-CN(2F); transition temperatures ( $^\circ\text{C}$ ) are on cooling from the isotropic liquid.<sup>5,33</sup> Green and red arrows indicate increased and decreased  $T_{\text{NF-N}}$  relative to the parent material, respectively, while a black dash indicates the absence of the  $\text{N}_F$  phase; note that the parent material does not display the  $\text{N}_F$  phase.



exhibit the  $N_F$  phase, a remarkable achievement given that this is not displayed in the parent compound. Variations in terminal chain length for one family of laterally trifluoromethylated materials show the same trend observed in other materials, namely that the stability of the  $N_F$  phase decreases as the aliphatic chain length is increased (Fig. 7).<sup>33</sup>

## Conclusions and outlook

The discovery of polar nematic order and ferroelectricity is the beginning of a new chapter in the history of soft matter science, and ranks among the most important discoveries in the 150 year history of liquid crystals. With our understanding of this new phase of matter in its infancy, efforts to understand the rich physics of ferroelectric nematics will no doubt be the major topic in liquid crystal research in the coming decades. Such investigations are reliant on the development of new materials and design rules for  $N_F$  materials, and in understanding how changes at a molecular level affects the bulk properties of the resulting material. Much as the promise display devices motivated the synthesis of room temperature nematic materials from the 1950s onwards, the unique combination of properties offered by ferroelectric nematics provide a clear pull towards applications; for example, tunable dielectrics, solution processable ferroelectrics, sensors. The number of materials known to exhibit the  $N_F$  phase is growing exponentially and is no longer restricted to the RM/DIO type-core structures; indeed, the observation of polar nematic order in oligomeric and polymeric materials suggests that spontaneous polar order is in fact a general phenomenon. As the pool of known  $N_F$  materials widens, our ability to tuning physical properties (transition temperatures, spontaneous polarization, and so on) through mixture formulation grows, enabling the tailoring of material properties towards specific applications and/or experiments. All the while, in unison with materials design and synthesis, theoretical understanding of this nascent phase of matter is evolving rapidly. The future of polar and ferroelectric nematics looks extremely bright.

## Conflicts of interest

There are no conflicts to declare.

## Acknowledgements

RJM acknowledges funding from UKRI via a Future Leaders Fellowship, grant no. MR/W006391/1.

## References

- 1 M. Bremer, P. Kirsch, M. Klasen-Memmer and K. Tarumi, *Angew. Chem., Int. Ed.*, 2013, **52**, 8880–8896.
- 2 M. Born, *Sitzungsber. Preuss. Akad. Wiss.*, 1916, **30**, 614–650.
- 3 F. C. Frank, *Discuss. Faraday Soc.*, 1958, **25**, 19–28.
- 4 H. Pleiner and H. R. Brand, *Europhys. Lett.*, 1989, **9**, 243–249.
- 5 R. J. Mandle, S. J. Cowling and J. W. Goodby, *Chem. – Eur. J.*, 2017, **23**, 14554–14562.
- 6 H. Nishikawa, K. Shiroshita, H. Higuchi, Y. Okumura, Y. Haseba, S. I. Yamamoto, K. Sago and H. Kikuchi, *Adv. Mater.*, 2017, **29**, 1702354.
- 7 A. Mertelj, L. Cmok, N. Sebastian, R. J. Mandle, R. R. Parker, A. C. Whitwood, J. W. Goodby and M. Copic, *Phys. Rev. X*, 2018, **8**, 041025.
- 8 X. Chen, E. Korblova, D. Dong, X. Wei, R. Shao, L. Radzihovsky, M. A. Glaser, J. E. Maclennan, D. Bedrov, D. M. Walba and N. A. Clark, *Proc. Natl. Acad. Sci. U. S. A.*, 2020, **117**, 14021–14031.
- 9 R. J. Mandle, N. Sebastián, J. Martínez-Perdiguero and A. Mertelj, *Nat. Commun.*, 2021, **12**, 4962.
- 10 N. Sebastian, L. Cmok, R. J. Mandle, M. R. de la Fuente, I. Drevensek Olenik, M. Copic and A. Mertelj, *Phys. Rev. Lett.*, 2020, **124**, 037801.
- 11 C. L. Folcia, J. Ortega, R. Vidal, T. Sierra and J. Etxebarria, *Liq. Cryst.*, 2022, 1–8, DOI: [10.1080/02678292.2022.2056927](https://doi.org/10.1080/02678292.2022.2056927).
- 12 N. Sebastian, R. J. Mandle, A. Petelin, A. Eremin and A. Mertelj, *Liq. Cryst.*, 2021, **48**, 2055–2071.
- 13 M. Tibor Máthé, Á. Buka, A. Jáklí and P. Salamon, ArXiv e-prints, 2022, arXiv:2201.07556.
- 14 F. Caimi, G. Nava, R. Barboza, N. A. Clark, E. Korblova, D. M. Walba, T. Bellini and L. Lucchetti, *Soft Matter*, 2021, **17**, 8130–8139.
- 15 O. D. Lavrentovich, *Proc. Natl. Acad. Sci. U. S. A.*, 2020, **117**, 14629–14631.
- 16 R. J. Mandle, S. J. Cowling and J. W. Goodby, *Phys. Chem. Chem. Phys.*, 2017, **19**, 11429–11435.
- 17 H. Nishikawa and F. Araoka, *Proc. Natl. Acad. Sci. U. S. A.*, 2021, **33**, 2101305.
- 18 X. Zhao, J. Zhou, J. Li, J. Kougo, Z. Wan, M. Huang and S. Aya, *Proc. Natl. Acad. Sci. U. S. A.*, 2021, **118**, e2111101118.
- 19 X. Chen, E. Korblova, M. A. Glaser, J. E. Maclennan, D. M. Walba and N. A. Clark, *Proc. Natl. Acad. Sci. U. S. A.*, 2021, **118**, e2104092118.
- 20 D. Pocięcha, R. Walker, E. Cruickshank, J. Szydłowska, P. Rybak, A. Makal, J. Matraszek, J. M. Wolska, J. M. D. Storey, C. T. Imrie and E. Gorecka, ArXiv e-prints, 2021, arXiv:2112.11887.
- 21 R. J. Mandle, S. J. Cowling and J. W. Goodby, *Liq. Cryst.*, 2021, **48**, 1780–1790.
- 22 I. Dozov, *Europhys. Lett.*, 2001, **56**, 247–253.
- 23 M. Cestari, S. Diez-Berart, D. A. Dunmur, A. Ferrarini, M. R. de la Fuente, D. J. Jackson, D. O. Lopez, G. R. Luckhurst, M. A. Perez-Jubindo, R. M. Richardson, J. Salud, B. A. Timimi and H. Zimmermann, *Phys. Rev. E: Stat., Nonlinear, Soft Matter Phys.*, 2011, **84**, 031704.
- 24 D. Chen, J. H. Porada, J. B. Hooper, A. Klitnick, Y. Shen, M. R. Tuchband, E. Korblova, D. Bedrov, D. M. Walba, M. A. Glaser, J. E. Maclennan and N. A. Clark, *Proc. Natl. Acad. Sci. U. S. A.*, 2013, **110**, 15931–15936.
- 25 E. T. Samulski, A. G. Vanakaras and D. J. Photinos, *Liq. Cryst.*, 2020, **47**, 2092–2097.
- 26 B. R. Ratna, S. K. Prasad, R. Shashidhar, G. Heppke and S. Pfeiffer, *Mol. Cryst. Liq. Cryst.*, 1985, **124**, 21–26.
- 27 R. Shashidhar, B. R. Ratna and S. K. Prasad, *Mol. Cryst. Liq. Cryst.*, 1984, **102**, 105–111.



- 28 J. Li, H. Nishikawa, J. Kougo, J. Zhou, S. Dai, W. Tang, X. Zhao, Y. Hisai, M. Huang and S. Aya, *Sci. Adv.*, 2021, **7**, eabf5047.
- 29 R. Saha, P. Nepal, C. Feng, M. Sakhawat Hossein, J. T. Gleeson, S. Sprunt, R. J. Twieg and A. Jakli, arXiv e-prints, 2021, arXiv:2104.06520.
- 30 S. Brown, E. Cruickshank, J. M. D. Storey, C. T. Imrie, D. Pocięcha, M. Majewska, A. Makal and E. Gorecka, *ChemPhysChem*, 2021, **22**, 2506–2510.
- 31 T. Masukawa, *Orthoester derivative, liquid crystal composition and liquid crystal display device*, *China Pat.*, CN103443104B, 2017.
- 32 P. Kirsch, W. Binder, A. Hahn, K. Jährling, M. Lenges, L. Lietzau, D. Maillard, V. Meyer, E. Poetsch, A. Ruhl, G. Unger and R. Fröhlich, *Eur. J. Org. Chem.*, 2008, 3479–3487.
- 33 J. Li, Z. Wang, M. Deng, Y. Zhu, X. Zhang, R. Xia, Y. Song, Y. Hisai, S. Aya and M. Huang, *Giant*, 2022, **11**, 100109.
- 34 E. J. Corey and N. Raju, *Tetrahedron Lett.*, 1983, **24**, 5571–5574.
- 35 Z. X. Li Ming, M. Guo Liang, L. Wenhai, Z. Lei, W. Jin and H. Ruimao, *Liquid crystal compound containing 5-cyclobutyl-1,3-dioxy cyclohexane structure, preparation method and applications thereof*, *China Pat.*, CN105481824A, 2014.
- 36 L. C. Han Yaohua, D. Xingli and G. Linlin, *A kind of compound, liquid-crystal composition and liquid crystal display*, *China Pat.*, CN105669595B, 2015.
- 37 P. Rudquist, *Sci. Rep.*, 2021, **11**, 24411.
- 38 A. Manabe, M. Bremer and M. Kraska, *Liq. Cryst.*, 2021, **48**, 1079–1086.
- 39 Y. Song, J. Li, R. Xia, H. Xu, X. Zhang, H. Lei, W. Peng, S. Dai, S. Aya and M. Huang, *Phys. Chem. Chem. Phys.*, 2022, DOI: [10.1039/D2CP01110G](https://doi.org/10.1039/D2CP01110G).
- 40 S. Dai, J. Li, J. Kougo, H. Lei, S. Aya and M. Huang, *Macromolecules*, 2021, **54**, 6045–6051.
- 41 H. Nishikawa, K. Sano and F. Araoka, *Nat. Commun.*, 2022, **13**, 1142.
- 42 J. Li, R. Xia, H. Xu, J. Yang, X. Zhang, J. Kougo, H. Lei, S. Dai, H. Huang, G. Zhang, F. Cen, Y. Jiang, S. Aya and M. Huang, *J. Am. Chem. Soc.*, 2021, **143**, 17857–17861.

